Geotechnical Engineering Journal of the SEAGS & AGSSEA Vol 41 No.4 December 2010 ISSN0046-5828

Response of Porous Seabed to Dynamic Loadings

D-S Jeng[1, 2,*], X L Zhou[1], X D Luo[2], JH Wang[1], J Zhang[2] and F. P. Gao[3]
[1] *Centre for Marine Geotechnics Research, Department of Civil Engineering, Shanghai Jiao Tong University, China*
[2] *Division of Civil Engineering, University of Dundee, Dundee, DD1 4HN, Scotland, UK*
[3]*Key Laboratory for Hydrodynamics and Ocean Engineering Institute of Mechanics, Chinese Academy of Sciences, Beijing 100190 China.*
* *Corresponding author, e-mail*:d.jeng@dundee.ac.uk

ABSTRACT: The evaluation of the seabed response, including pore pressure, effective stresses and shear stresses, is particularly important for coastal geotechnical engineers involved in the design of foundation around marine structures. This paper consists of two components. The first component focuses on analytical approximation for the seabed response, in which a new analytical solution for the seabed response due to combined wave and current loading is presented. Both transient and residual mechanisms are considered. Based on the new analytical solution, the effects of currents on the seabed response are examined and a modified J-S curve is presented. The second component will present an integrated model for ocean waves propagating over a submerged coastal structure. In the new model, Navier-Stoke equations, Biot's poro-elastic theory, and structural mechanics theory are solved for wave propagation, seabed response and structure deformation, respectively. The new feature of this model is to integrate wave, soil and structure modes into one model within COMSOL Multiphysics environments. In this part, we first present the model of ocean wave generation over a porous seabed. Then we further consider two coastal engineering problems: (1) ocean waves propagating over a submerged breakwater on a porous seabed; and (2) waves over a deformable structure on a porous seabed, which can be applied to wave energy converter.

1. INTRODUCTION

The phenomenon of pore pressure within a seabed is an important feature in coastal engineering problems such as the stability of breakwaters and the sinking or uplifting of pipelines. It is well known that ocean waves/currents can generate significant dynamic pressures on the sea floor. This dynamic pressure further induces pore-water pressure and effective stresses within the seabed. With excess pore pressure and diminishing vertical effective stress, part of the seabed may become unstable or even liquefied. Once liquefaction occurs, the soil particles are likely to be carried away as a fluid by any prevailing bottom current or mass transport owing to the natural loadings such as waves and currents.

This paper consists of two components: (i) analytical approximation for the seabed response due to dynamic loading (including waves and currents); and (ii) integrated numerical model for waves propagating over a porous seabed around marine structures.

Two mechanisms of the seabed response have been observed in the field measurements and laboratory experiments, depending upon how the excess pore pressure is generated (Nago et. al, 1993). One is caused by the residual or progressive nature of the excess pore pressure, which appears in the initial stage of cyclic loading. This type of soil response is similar to that induced by earthquakes, caused by the buildup of excess pore pressure (Seed and Rahman, 1978). The other, generated by transient or oscillatory excess pore pressures, is accompanied by the damping of amplitude and phase lag in the pore pressure, and appears as a periodic response to each wave (Yamamoto et. al, 1978; Jeng and Hsu, 1996).

Numerous investigations of the wave-induced transient soil response have been reported, based on different assumptions of relative rigidity for pore fluid and soil skeleton. Among these, Yamamoto et al. (1978) developed an analytical solution for the water waves/soil interaction problem within a hydraulically isotropic seabed of infinite thickness. For a fully saturated seabed, the soil response was also found to be independent of the soil permeability and no phase lag was observed. On the other hand, pore pressure attenuates rapidly with a phase lag in an unsaturated seabed. Details of previous investigations of wave–seabed–structure interactions were summarized in Jeng (2003).

Residual mechanisms of wave-induced pore pressure have been investigated since Seed and Rahman (1978). Dynamic wave pressures that vary harmonically in space and time will generate cyclic shear stresses in the soil that can cause the contraction of relatively loose soils and in turn lead to an increase in the mean excess pore-water pressure if drainage is impeded. These mean pore pressures are not uniquely related to instantaneous values of the wave-induced stresses, but depend on the accumulated action of the cyclic loading and the rate of pore pressure dissipation. Under this action, liquefaction may develop in un-drained or poorly drained conditions. Some recent investigations of this mechanism were carried out by numerous researchers (Sumer and Cheng, 1999; Sumer and Fredsoe, 2002; Sassa and Sekiguchi, 1999; Jeng and Seymour, 2007).

It is noted that all aforementioned investigations have only considered wave loading, totally ignored another important natural loading-ocean currents. In §2, the seabed response within a porous seabed will be re-examined by considering the combined loadings of waves and currents. Both transient and residual mechanisms will be considered in this study. Based on the newly analytical solutions, a simplified approach for the predictions of liquefaction will be proposed for engineering practice.

Marine structures on a porous seabed have been widely constructed for the coastal protections, oil production transport and offshore wind farm foundation. The existence of these structures (such as breakwaters, vertical walls, pipelines and mono-piles, etc.) will largely interact with the water surface waves, and consequently affect the wave-induced seabed responses around the marine structures.

In the past few decades, considerable effort has been devoted to the wave-soil-structure interaction (WSSI) phenomenon. The major reason for this growing interest is that many marine structures have been damaged by the wave-induced seabed response, rather than from the construction deficiencies (Christian et. al, 1974; Smith and Gordon, 1983; Lundgren et. al, 1989). To have a better understanding of the functionality and stability of marine structures, the wave motion and seabed responses around these structures must be determined.

Numerous investigations for the wave-seabed-structure interactions have been carried out since the 1980s. A detailed review of previous research in the area can be found in (Jeng, 2003). Most of them have been focused on the individual approaches (Mase et. al, 1994; Jeng, et. al, 2000; Magda, 2000), rather than an integrations of wave, seabed and structure models. However, the phenomenon of the wave-seabed-structure interactions will not been fully captured without a consideration of all components together.

In §3, based on COMSOL Multiphysics, is to develop an integrated model for ocean waves propagating over a marine structure on a porous seabed.

2. WAVE/CURRENT INDUCED SEABED RESPONSE

2.1 Wave field

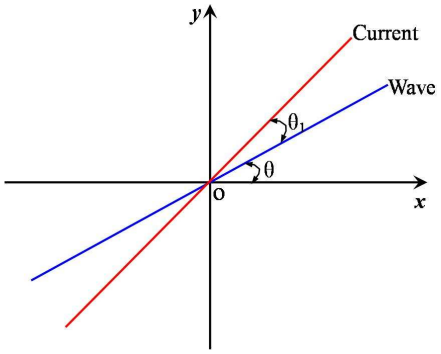

(a) Plan view

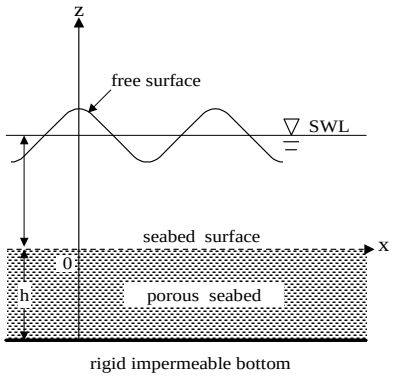

(b) Cross view

Figure 1. Sketch of wave-current propagating over a seabed

Considering combining wave and current loadings along a porous seabed, as shown in Fig. 1, the angle between waves and currents are denoted as θ_1, and angle between the direction of wave propagation and the x-direction is θ. Based on potential flow theory, the velocity potential (ϕ) satisfies the conservation of mass, leads to,

$$\nabla^2\phi = 0\,, \tag{1}$$

in which the velocity of fluid is defined as

$$(u,v,w) = -\nabla\phi \tag{2}$$

The velocity potential (ϕ) in (1) satisfies the free surface boundary conditions,

- Dynamic free surface boundary conditions:

$$-\frac{\partial\phi}{\partial t} + g(\eta + d) + \frac{1}{2}\left[\left(\frac{\partial\phi}{\partial x}\right)^2 + \left(\frac{\partial\phi}{\partial y}\right)^2 + \left(\frac{\partial\phi}{\partial z}\right)^2\right] = C \tag{3}$$

where η is the water elevation, d is water depth, and C is the Bernoullis' coefficients.

- Kinematic free surface boundary condition:

$$-\frac{\partial\phi}{\partial z} = \frac{\partial\eta}{\partial t} - \frac{\partial\phi}{\partial x}\frac{\partial\eta}{\partial x} - \frac{\partial\phi}{\partial y}\frac{\partial\eta}{\partial y} \tag{4}$$

The velocity potential and wave profile can be obtained by solving (1) with linearised (3) and (4), and expressed as:

$$\eta = \frac{H}{2}\cos(mkx + nky - \omega t) \tag{5}$$

$$\phi = -U_0\left[(mm_1 - nn_1)x + (nm_1 + mn_1)y\right] - \frac{gH\cosh kz}{2\omega(1 - \frac{U_0 m_1 k}{\omega})\cosh kd}\sin(mkx + nky - \omega t) \tag{6}$$

where k is the wave number, and $m = \cos\theta$, $n = \sin\theta$, $m_1 = \cos\theta_1$, $n_1 = \sin\theta_1$. The detailed derivations can be found in appendix.

The wavelength can be determined by the wave dispersion relation given by:

$$\left(\omega - m_1 U_0 k\right)^2 = gk\tanh kd \tag{7}$$

It is noted that an addition variable "m_1" appears in (7), which only exists for the combing wave and current loadings. For the case with waves only, m_1=0.

Based on the above potential theory for combined wave and current loading, the dynamic wave pressure can be expressed as:

$$P_d = \frac{\rho g H}{2}\frac{\cosh kz}{\cosh kd}\cos(mkx + nky - \omega t)\,. \tag{8}$$

2.2 Poro-elastic model-transient mechanism

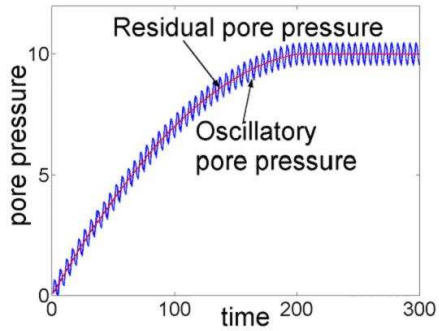

Figure 2. Mechanism of wave-induced pore pressure (not in scale)

For the problem of wave-seabed interaction, as shown in Fig. 2, the Biot consolidation theory (Biot, 1941) has been generally adopted to model the dynamic response of marine sediments for various applications. In general, the wave-induced pore pressure within marine sediments consists of two components: oscillatory ($\tilde{p}$) and residual ($\bar{p}$) mechanisms, which can be expressed as (see Fig. 2):

$$p = \tilde{p} + \bar{p}\,, \tag{9}$$

where p is the pore water pressure, $\tilde{p}$ represents the oscillatory pore pressure that leads to momentary liquefaction, while u represents the period-averaged pore pressure that leads to residual liquefaction, and is defined by:

$$\bar{p} = \frac{1}{T}\int_t^{t+T} p\,dt\,, \tag{10}$$

where T is the wave period and t is the time.

For the transient soil response in a saturated seabed, the Biot's consolidation equation is commonly used as the governing equation, i.e.,

$$\frac{\partial^2 p}{\partial x^2}+\frac{\partial^2 p}{\partial y^2}+\frac{\partial^2 p}{\partial z^2}-\frac{\gamma_w}{k}\frac{\partial \varepsilon}{\partial t}=0 \tag{11}$$

where the volume strain is defined by:

$$\varepsilon=\frac{\partial u}{\partial x}+\frac{\partial v}{\partial y}+\frac{\partial w}{\partial z} \tag{12}$$

The equations of force balance can be expressed as:

$$\frac{\partial \sigma_x'}{\partial x}+\frac{\partial \tau_{xy}}{\partial y}+\frac{\partial \tau_{xz}}{\partial z}=\frac{\partial p}{\partial x} \tag{13}$$

$$\frac{\partial \tau_{xy}}{\partial x}+\frac{\partial \sigma_y'}{\partial y}+\frac{\partial \tau_{yz}}{\partial z}=\frac{\partial p}{\partial y} \tag{14}$$

$$\frac{\partial \tau_{xy}}{\partial x}+\frac{\partial \tau_{yz}}{\partial y}+\frac{\partial \sigma_z'}{\partial z}=\frac{\partial p}{\partial z} \tag{15}$$

Based on Biot's poro-elastic theory, the stress-strain relations are given as:

$$\sigma_x'=2G\left[\frac{\partial u}{\partial x}+\frac{\mu\varepsilon}{1-2\mu}\right], \tag{16}$$

$$\sigma_y'=2G\left[\frac{\partial v}{\partial y}+\frac{\mu\varepsilon}{1-2\mu}\right] \tag{17}$$

$$\sigma_z'=2G\left[\frac{\partial w}{\partial z}+\frac{\mu\varepsilon}{1-2\mu}\right], \tag{18}$$

$$\tau_{xz}=G\left[\frac{\partial u}{\partial z}+\frac{\partial w}{\partial x}\right] \tag{19}$$

$$\tau_{yz}=G\left[\frac{\partial v}{\partial z}+\frac{\partial w}{\partial y}\right], \tag{20}$$

$$\tau_{xy}=G\left[\frac{\partial u}{\partial y}+\frac{\partial v}{\partial x}\right] \tag{21}$$

Substituting (16)-(21) into (13)-(15), the equations of force balance can be expressed as:

$$G\nabla^2 u+\frac{G}{(1-2\mu)}\frac{\partial \varepsilon}{\partial x}=\frac{\partial p}{\partial x} \tag{22}$$

$$G\nabla^2 v+\frac{G}{(1-2\mu)}\frac{\partial \varepsilon}{\partial y}=\frac{\partial p}{\partial y} \tag{23}$$

$$G\nabla^2 w+\frac{G}{(1-2\mu)}\frac{\partial \varepsilon}{\partial z}=\frac{\partial p}{\partial z} \tag{24}$$

To solve the seabed response, including pore pressure and soil displacements, the following boundary conditions are required,

- At the surface of the seabed, the pore pressure is equal to the dynamic pressure generated by wave and currents, and the vertical effective normal stress and shear stresses vanish;

$$\sigma_z'=\tau_{xz}=\tau_{yz}=0 \tag{25}$$

$$p=\frac{\gamma_w H}{2\cosh\lambda d}\cos(mkx+nky-\omega t)=p_0\cos(mkx+nky-\omega t) \tag{26}$$

- At the bottom of the infinite seabed, the soil displacements and pore pressure vanish, i.e.,

$$u=v=w=p=0 \quad \text{as} \quad z\to-\infty \tag{27}$$

Following the framework proposed in Jeng (1997), the pore pressure and soil displacements in a saturated porous seabed due to combined wave and current loading can be expressed as:

$$\frac{2Gku}{p_0}=-mkz\exp(kz)\cos(mkx+nky-\omega t) \tag{28}$$

$$\frac{2Gkv}{p_0}=-nkz\exp(kz)\sin(mkx+nky-\omega t) \tag{29}$$

$$\frac{2Gkw}{p_0}=(kz-1)\exp(kz)\cos(mkx+nky-\omega t) \tag{30}$$

$$p=p_0\exp(kz)\cos(mkx+nky-\omega t) \tag{31}$$

Then, effective normal stresses and shear stresses can be expressed as:

$$\sigma_x'=-m^2 p_0 kz\exp(kz)\cos(mkx+nky-\omega t) \tag{32}$$

$$\sigma_y'=-n^2 p_0 kz\exp(kz)\cos(mkx+nky-\omega t) \tag{33}$$

$$\sigma_z'=p_0 kz\exp(kz)\cos(mkx+nky-\omega t) \tag{34}$$

$$\tau_{xz}=-mp_0\lambda z\exp(\lambda z)\cos(m\lambda x+n\lambda y-\omega t) \tag{35}$$

$$\tau_{yz}=-np_0 kz\exp(kz)\cos(mkx+nky-\omega t) \tag{36}$$

$$\tau_{xy}=-mnp_0 kz\exp(kz)\cos(mkx+nky-\omega t) \tag{37}$$

2.3 Poro-elastic model-resident mechanism

The residual pore pressure ($\bar{p}$) in a homogenous, isotropic soil can be derived from the one-dimensional Biot's consolidation equation:

$$\frac{\partial \bar{p}}{\partial t}=c_v\frac{\partial^2 \bar{p}}{\partial z^2}+f(z) \tag{38}$$

where f is the mean accumulation pore pressure source term associated with the surface water waves. In (38), c_v is the coefficient of consolidation, given by:

$$c_v=\frac{2GK(1-\mu)}{\gamma_w(1-2\mu)} \tag{39}$$

The source term, $f(z)$, is defined by (Seed and Rahman, 1978):

$$f=\frac{\sigma_0'}{T}\left[\frac{|\tau|}{\alpha\sigma_0'}\right]^{1/\beta} \tag{40}$$

in which the amplitude of shear stress is determined by oscillatory seabed response,

$$|\tau|=\sqrt{\tau_{xz}^2+\tau_{yz}^2+\tau_{xy}^2}=\sqrt{(1+m^2n^2)}\,p_0 kz \tag{41}$$

Combing (40) and (41)，the source term can be expressed as:

$$f(z)=Az\exp(-kz) \tag{42}$$

where,

$$A=\frac{\gamma'(1+2K_o)}{3T}\left(\frac{3\sqrt{(1+m^2n^2)}p_0k}{\alpha(1+2K_o)\gamma'}\right)^{1/\beta} \tag{43}$$

$$\lambda=\frac{k}{\beta} \quad \text{and} \quad \gamma'=\gamma_s-\gamma_w \tag{44}$$

To solve (38), the following boundary and initial conditions are required:

$$\bar{p}(0,t)=\bar{p}(z,0)=0\,, \text{ and } \bar{p}(\infty,t)=0\,. \tag{45}$$

Then, the residual pore pressure is calculated using a Laplace transformation as:

$$\bar{p}=\frac{2A}{c_v\lambda^3}\left[1-\left(\frac{\lambda z}{2}+1\right)\exp(-\lambda z)-\frac{1}{\pi}\int_0^{\infty}\frac{\exp(-rc_v\lambda^2 t)}{r(r+1)^2}\sin(\sqrt{r}\lambda z)dr\right] \tag{46}$$

2.4 Effects of currents on the wave-induced soil response

One of new contributions of this study is the consideration of ocean currents in the existing seabed response model. Most previous models for the wave-seabed interactions have been limited to wave loading only. In this paper, we consider an additional loading from ocean currents. In this section, we first investigate the effects of ocean currents on the wave-induced soil response in a porous seabed.

The vertical distributions of the maximum amplitude of the wave-induced soil response versus the soil depth for various current velocities are illustrated in Figs. 3 to 5. The input data for numerical examples presented in the figures are tabulated in Table 1. As shown in the figures, the vertical displacement (w) is greater than horizontal soil displacements (u and v), and the vertical effective normal stress (σ_z') is greater than horizontal normal stresses (σ_x' and σ_y'). Furthermore, the vertical shear stress (τ_{xz}) is greater than other shear stresses (τ_{yz} and τ_{xy}).

One of new features of this solution is the inclusion of currents. Figs. 6 and 7 illustrate the vertical distributions of the pore pressures and vertical effective normal stresses for various current velocities. In the figures, the pore pressure and vertical effective normal stress increases as the velocity of currents increases. It is noted that the special case, $U_0=0$, is the case without currents, i.e., the solution of Hsu et al. (1883).

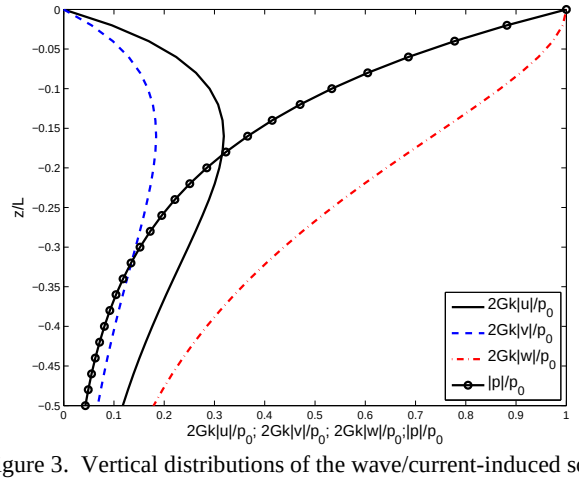

Figure 3. Vertical distributions of the wave/current-induced soil displacements and pore pressure in a porous seabed

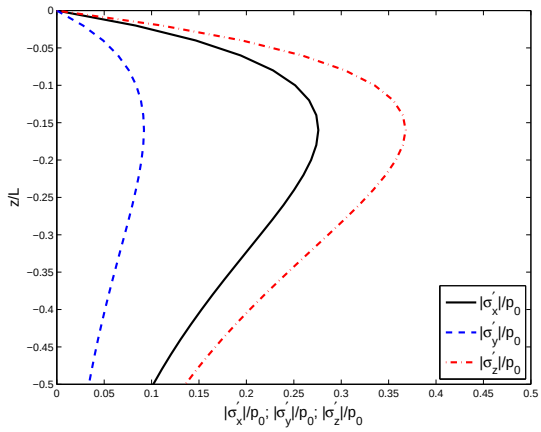

Figure 4. Vertical distributions of the wave/current-induced effective normal stresses in a porous seabed

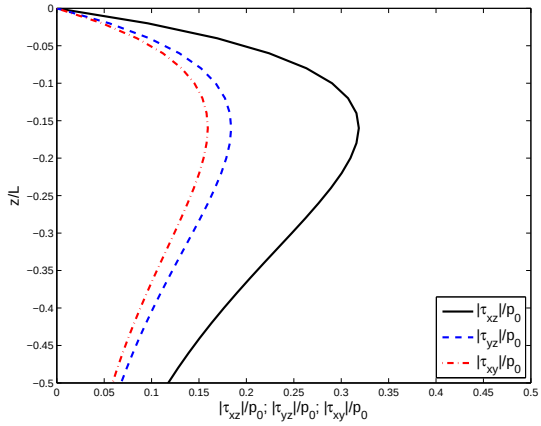

Figure 5. Vertical distributions of the wave/current-induced shear stresses in a porous seabed

Table 1. Input data for numerical examples

Wave Characteristics	
Wave period	12.5 sec
Water depth	10 m
Wave height	2 m
Current velocity	3 m/sec or various
Wave obliquity (θ)	30°
Angle between wave and currents (θ_1)	60°
Soil Characteristics	
Coefficient of consolidation	0.01
Residual parameter α	0.246
Residual parameter β	0.8
Unit weight of soil	26500 N/m^3

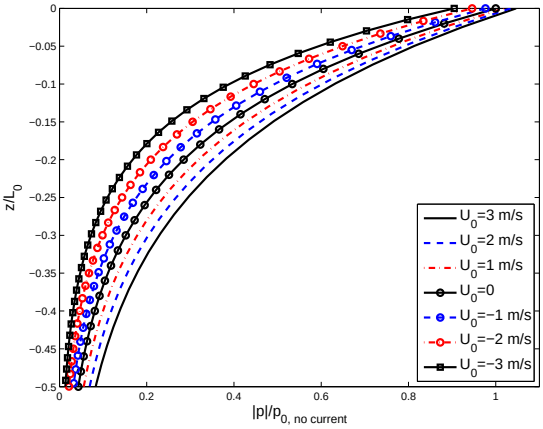

Figure 6. Vertical distributions of the wave/current-induced pore pressure in a porous seabed for various current velocities

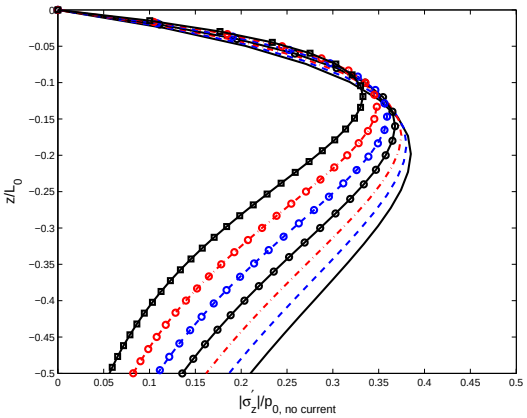

Figure 7. Vertical distributions of the wave/current-induced vertical effective normal stresses in a porous seabed for various current velocities (The legend is the same as that in Fig. 6)

2.5 Simplified formulation for wave-induced liquefaction

For engineers, the most important task is to examine where liquefaction will occur and how deep it is. The well-known criterion of residual liquefaction is:

$$\frac{P_{res}}{\sigma_0'} = 1 \tag{47}$$

which results in:

$$\bar{p}(z,\infty) = \frac{2A}{c_v\lambda^3}\left[1-\left(\frac{\lambda z_L}{2}+1\right)\exp(-\lambda z_L)\right] = \sigma_0' = \frac{(1+2K_o)}{3}\gamma' z_L \tag{48}$$

Let

$$B = \frac{(1+2K_o)\gamma' c_v\lambda^2}{6A}, \tag{49}$$

We have:

$$\left[1-\left(\frac{\lambda z_L}{2}+1\right)\exp(-\lambda z_L)\right] = B\lambda z_L \tag{50}$$

Based on (50), the relationship the maximum liquefied depth (z_L) and the parameter B is presented in Fig. 8. This relation, so-called J-S curve, was first proposed by Jeng and Seymour (2007) for the case of wave loading. In Fig. 8, the currents are included. For engineering applications, given waves, currents and soil conditions, we can determine the parameter B from (49). The maximum liquefied depth can then be easily determined from Fig. 8.

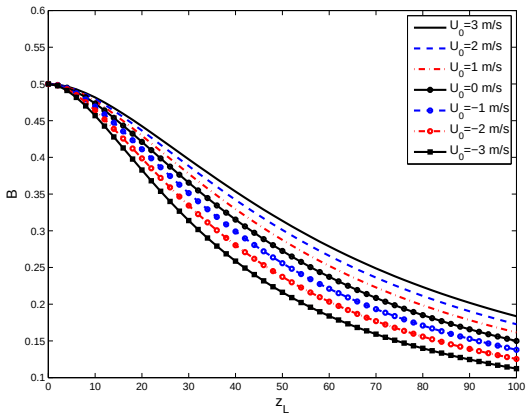

Figure 8. Modified J(eng)-S(eymour) curve fro wave/current induced liquefaction

3. INTEGRATED MODEL FOR WAVE-SEABED-STRUCTURE INTERACTIONS

An integrated model for WSSI is developed in this section. An assumption is made that the poro-elastic deformations in seabed are very small and do not affect the wave transformations or its induced pressure on the surface of the poro-elastic seabed (Mizutani et. al, 1998). This assumption simplifies the boundary conditions at the seabed interface where the water pressure and shear stress calculated from the wave field are passed into the seabed. This integrated model includes three main components: (i) wave mode on the basis of the Navier-Stokes (N-S) equations; (ii) seabed mode on the basis of the Biot's consolidation equations with poro-elastic theory; and (iii) structure mode on the basis of structural mechanics theory.

3.1 Wave mode

Navier-Stokes (N-S) equations are utilized to describe motion of the water liquid phase. Starting with the momentum balance in terms of stresses, the generalized equations in terms of transport properties and velocity gradients are:

$$\rho\frac{\partial\vec{u}}{\partial t} - \nabla\cdot[\eta(\nabla\vec{u}+(\nabla\vec{u})^T)] + \rho(\vec{u}\cdot\nabla)\vec{u} + \nabla p_f = \vec{F} \tag{51}$$

$$\nabla\cdot\vec{u} = 0 \tag{52}$$

where η is the dynamic viscosity of fluid, ρ is the fluid density, $\vec{u}$ is the velocity field, p_f is the pressure, t is the time, and $\vec{F}$ is a volume force such as gravity.

3.2 Seabed mode

The consolidation equation for the flow of a compressible pore fluid in a compressible porous medium can be given as (Christian et. al, 1974):

$$\nabla\cdot(K\nabla p) - \gamma_w n'\beta\frac{\partial p}{\partial t} = \gamma_w\frac{\partial\varepsilon_s}{\partial t} \tag{53}$$

where p is the pore pressure, K is the permeability matrix of the soil, γ_w is the unit weight of pore water, n' is the soil porosity, and $\varepsilon_s = \nabla\cdot\vec{u}_s$ (where $\vec{u}_s$ is the soil displacement) is the volume strain of soil matrix. The compressibility of pore fluid (β) is defined as:

$$\beta = \frac{1}{K_w} + \frac{1-S}{P_{w0}} \tag{54}$$

in which K_w is the true modulus of elasticity of water (taken as 2×10^9N/m^2), P_{w0} is the absolute water pressure and S is the degree of saturation.

The relationships between soil displacement and pore pressure are given as:

$$G\nabla^2\vec{u}_s + \frac{G}{1-2\mu_s}\nabla\varepsilon_s = \nabla p \tag{55}$$

where G is the shear modulus related to the Young's modulus (E) and the Poisson's ratio (μ_s) in the form of $E/(2(1+\mu_s))$.

3.3 Structure mode

Based on the small-displacement assumption, the relationships between strain components and displacement at a point of marine structure are given as follows:

$$\varepsilon_x = \frac{\partial u_m}{\partial x}, \tag{56}$$

$$\varepsilon_{xy} = \frac{1}{2}\left(\frac{\partial u_m}{\partial y} + \frac{\partial v_m}{\partial x}\right), \tag{57}$$

$$\varepsilon_y = \frac{\partial v_m}{\partial y}, \tag{58}$$

$$\varepsilon_{yz} = \frac{1}{2}\left(\frac{\partial v_m}{\partial z} + \frac{\partial w_m}{\partial y}\right), \tag{59}$$

$$\varepsilon_z = \frac{\partial w_m}{\partial z}, \tag{60}$$

$$\varepsilon_{xz} = \frac{1}{2}\left(\frac{\partial u_m}{\partial z} + \frac{\partial w_m}{\partial x}\right) \tag{61}$$

The strain tensor ε and stress tensor σ are:

$$\varepsilon = \begin{bmatrix} \varepsilon_x & \varepsilon_{xy} & \varepsilon_{xz} \\ \varepsilon_{yx} & \varepsilon_y & \varepsilon_{yz} \\ \varepsilon_{zx} & \varepsilon_{zy} & \varepsilon_z \end{bmatrix}, \quad \sigma = \begin{bmatrix} \sigma_x & \tau_{xy} & \tau_{xz} \\ \tau_{yx} & \sigma_y & \tau_{yz} \\ \tau_{zx} & \tau_{zy} & \sigma_z \end{bmatrix}, \tag{62}$$

The stress-strain relationship for linear conditions reads:

$$\sigma = D_m \varepsilon \tag{63}$$

where D_m is the elasticity matrix.

The structural mechanics theory in this study is based on a weak formulation of the equilibrium equations expressed in the global stress components.

$$-\nabla \cdot \sigma = \vec{F}_m \tag{64}$$

in which $\vec{F}_m$ denotes the volume forces (body forces).

3.4 Wave generation

In this numerical model, a piston wave generator is used. According to (Dean and Dalrymple, 1991), the expression of the movement of the wave maker is:

$$U(t) = \frac{S\omega}{2}\cos\omega t \tag{65}$$

where, the S and ω are the stroke and the frequency of the wave maker respectively. The fluid evaluation $\eta(x)$ is donated as:

$$\eta(x) = \frac{i\omega}{g}\left(C_0 e^{ik_0 x} + \sum_{m=1}^{\infty} C_m e^{-k_m x}\right) \tag{66}$$

$$C_0 = -\frac{\omega S}{N_0 k_0}\left[\frac{\tanh k_0 d}{k_0} + \frac{1}{dk_0^2 \cosh k_0 d} - \frac{1}{dk_0}\right] \tag{67}$$

$$C_m = -\frac{i\omega S}{N_m k}\left[\frac{\tanh k_m d}{k_m} - \frac{1}{dk^2 \cosh k_m d} + \frac{1}{dk_m}\right] \tag{68}$$

$$N_0 = \frac{1}{\cosh^2 k_0 d}\left(\frac{d}{2} + \frac{\sinh 2k_0 d}{4k_0}\right) \tag{69}$$

$$N_m = \frac{1}{\cosh^2 k_m d}\left(\frac{d}{2} + \frac{\sinh 2k_m d}{4k_m}\right) \tag{70}$$

where, the k_0 and k_m are the wave number. The depth and gravity of water are donated by d and g. The ratio of wave height (H) to stroke as following:

$$N_m = \frac{1}{\cosh^2 k_m d}\left(\frac{d}{2} + \frac{\sinh 2k_m d}{4k_m}\right) \tag{71}$$

In order to induce the wave energy dissipation and reduce the wave reflection from the right wall, a sponge (wave absorbing) boundary is needed. In this numerical model, in the last 100m on the right sides, the viscosity of the fluid is increased of approximately 10000times (with a smoothing exponential window).

3.5 Boundary conditions

When solving the governing equations, appropriate boundary conditions at external boundaries and internal interfaces for these three modes are required (see Fig. 9).

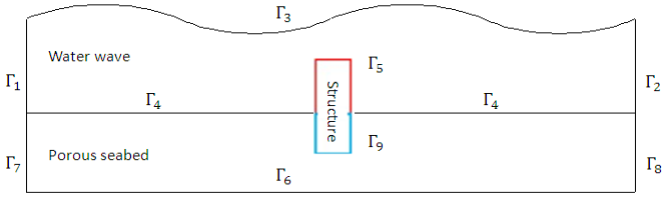

Figure 9. Locations for specification of boundary condition

In the wave mode, a piston wave maker is used in the left-hand-side boundary (Γ_1) of computational domain to generate wave and a sponge layer is located in the right-hand-side boundary (Γ_2) to avoid/reduce the wave reflection. Zero pressure is applied on the water free surface (Γ_3), while no-slip condition is adopted at the solid surface, such as sea floor (Γ_4) and surface of marine structure (Γ_5). In the case of a deformable structure, the impact of the structure deformation on wave motion is considered in term of a deformation of boundary shape (Γ_5).

In the seabed mode, it is commonly accepted that vertical effective normal stresses vanish at the seabed surface while the wave pressure and shear stresses obtained from wave mode are imposed as boundary conditions of seabed surface (Γ_4). In this study, the seabed is considered as a porous medium of a finite thickness and rests on an impermeable rigid bottom, indicating that zero displacements, zero gradient of pore pressure and no vertical flow occur at the horizontal bottom (Γ_6). When two side boundaries (Γ_7 and Γ_8) of seabed are far away from the concerned region (such as the region around a marine structure), they can be assumed to have zero displacement.

In the structure mode, the displacement and velocity at the surface (Γ_5) of a deformable structure are dominated by the wave pressure acting on the wave-structure interface. For the embedded part (Γ_9) of a structure, it is assumed to have same displacement and velocity as those of ambient soil (updated from seabed mode).

3.6 Numerical model

These three numerical modes are integrated by using COMSOL Multiphysics (3.5a version). The main features of COMSOL Multiphysics adopted to set up the integrated model are listed as follows:

(1) 2D space dimension;
(2) Plane strain mode of structural mechanics;

(3) Coefficient form of PDE mode for seabed mode;
(4) Incompressible Navier-Stokes mode of fluid dynamics;
(5) Arbitrary Lagrangian-Eulerian (ALE) method for mesh movement.

3.7 Wave-seabed Interaction

As a starting point, this integrated model is applied to predict the wave-seabed interaction without the inclusion of a marine. In the example, a computational domain with a length ($L = 200$ m) is used. The original of the Cartesian coordinate system is located at left-hand-size edge point of sea floor. The incident linear wave is generated with wave height ($H_w = 0.5$ m), wave period ($T = 6.0$ sec) and still water depth ($d = 10.0$ m). For the porous seabed, the seabed thickness, soil porosity, permeability and degree of saturation are taken as $d_s = 25.0$ m, $n' = 0.4$, $K = 0.01$ m/sec and $S = 0.98$, respectively.

Figure 10 shows an example of the distributions of wave-induced pore fluid pressure (p) and vertical effective normal stress (σ_z) within the seabed at time $t = 43.0$ sec. The magnitude of pore pressure decreases with depth increases. The magnitude of vertical effective normal stress increases firstly, and then decreases gradually. The comparisons between numerical results and analytical solutions of water elevation (Jeng, 1997), maximal pore water pressure and vertical effective normal stress (Magda, 2000) at cross-section $x = 100$ m are shown in Figs. 11 to 13, respectively. In general, there is a good agreement between numerical simulation and analytical theory. It is noted that the wave model used in the previous analytical solutions was based on the potential flow theory, which has no shear stresses along the seabed surface, while the present wave model was based on N-S equations.

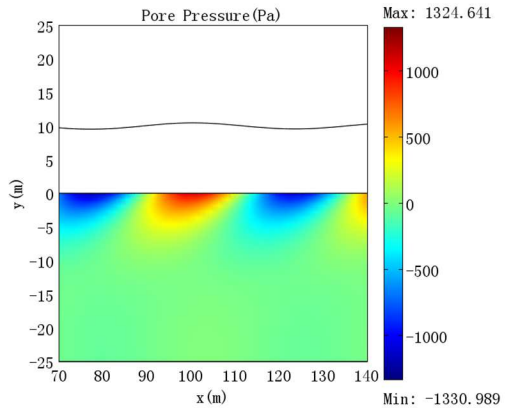

(a) pore pressure

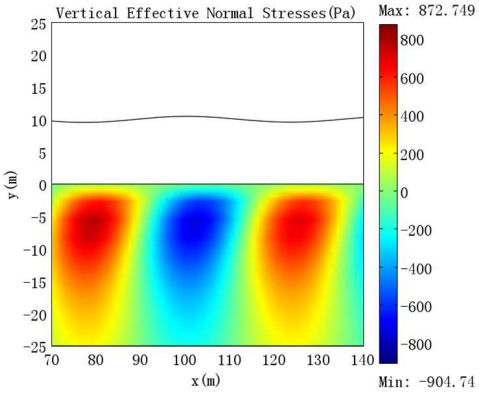

(b) Vertical effective normal stress

Figure 10. Distributions of (a) pore fluid pressure and (b) vertical effective normal stress with wave profile and velocity field at time $t = 43.0$ sec.

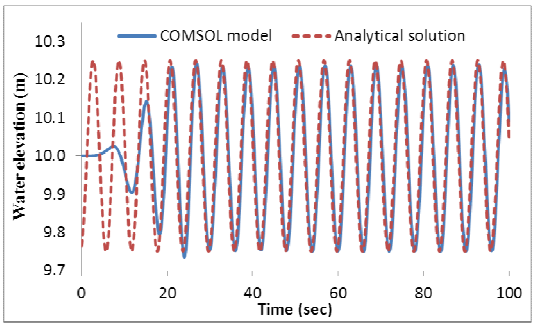

Figure 11. Comparison of simulated water elevation with analytical solution at the cross-section $x = 100$ m.

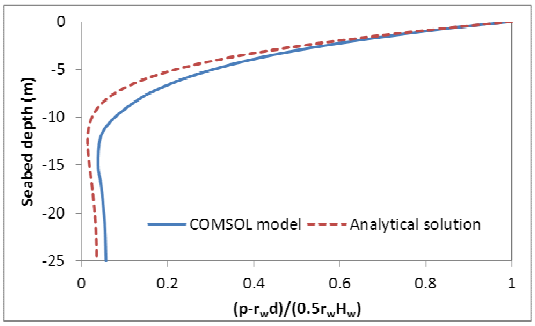

Figure 12. Comparison of simulated maximal pore pressure with analytical solution at the cross-section $x = 100$ m.

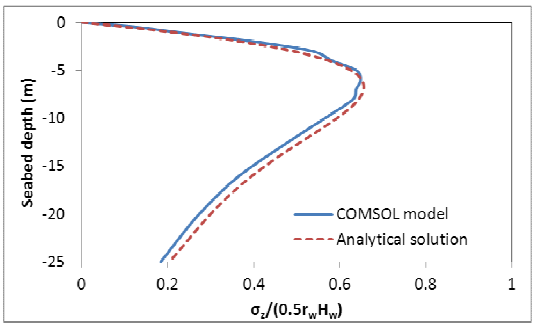

Figure 13. Comparison of simulated maximal vertical effective normal stress with analytical solution at the cross-section $x = 100$ m.

3.8 Wave-seabed Interaction around a Rigid Submerged Breakwater

In this section, a rigid, impermeable and submerged breakwater with a rectangular shape is considered, and its impacts on wave motion and seabed response are analyzed by the integrated model. The structure is 20 m wide and 3 m high, and its central point of bottom line is located at the point (105, 0). Figure 14 shows the distribution of the wave-induced pore fluid pressure around the structure at time $t = 43.0$ sec. As one can expect, the existence of structure can largely affect the wave motion around the submerged breakwater (see Fig. 15) and consequently leads to a different distribution of pore pressure from that without a marine structure (see Fig. 10(a) and Fig. 14). As shown in Fig. 15, an obvious wave deformation takes place due to wave-structure interaction when the wave is over the submerged breakwater.

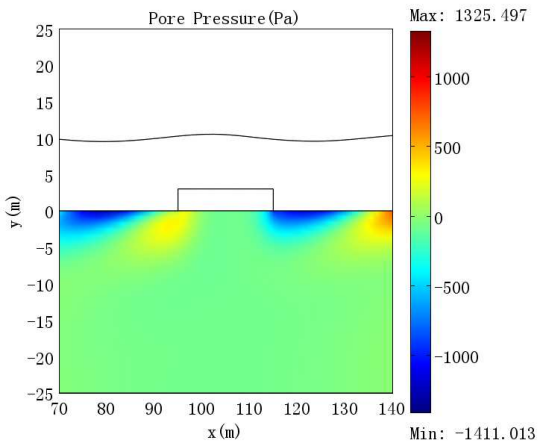

Figure 14. Distributions of the wave-induced pore pressure in a porous seabed at time $t = 43.0$ sec.

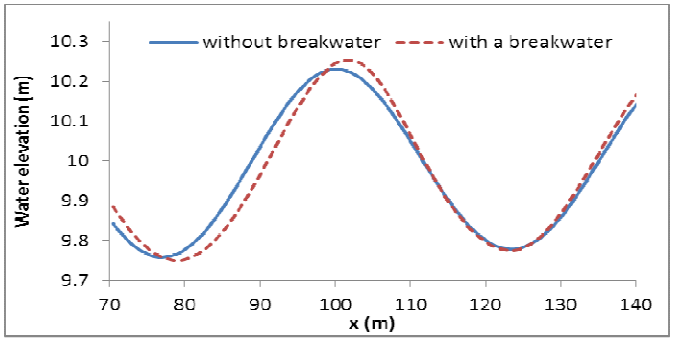

Figure 15. Comparsions of the simulated water elevation with and without the presence of a submerged breakwater at time $t = 43.0$ sec.

3.9 Wave-seabed Interaction around a Deformable Structure

This integrated model has also been used to study the wave propagation and seabed response around a deformable impermeable structure (such as wave energy converter). Two types of structure with different embedded depths are investigated, as depicted in Fig. 16. One is simply fixed on the sea floor with zero embedded depth, and the other is embedded into the seabed with an embedded depth of 2 m. The width and height above seabed are kept the same in these structures, and they are taken as 1 m and 5 m, respectively.

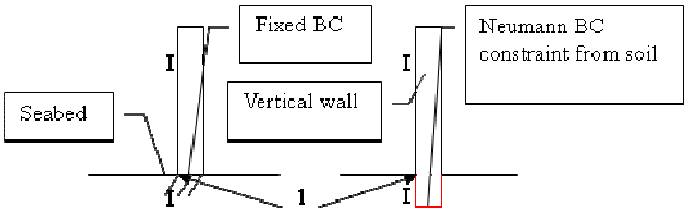

Figure 16. The sketch vertical structure and seabed model

Figure 17 illustrates the effects of structure obstacle on fluid velocity field, from which significant changes of velocity pattern around the structure can been observed. Furthermore, in this example, the wave crest arrives at the structure, which creates a positive pressure on the seabed surface, and result in compaction of the seabed.

Figure 18 shows the effects of embedded depth on the distribution of wave-induced pore pressure around foundation. As shown in the figure, there is about 2% of increment of the pore pressure amplitude in case 1, compare with case 2. The comparison indicates the embedded part of structure may disturb/block the development of pore pressure. This implies that the embedded pile will reduce the pore pressure, and enhance the stability of the structure.

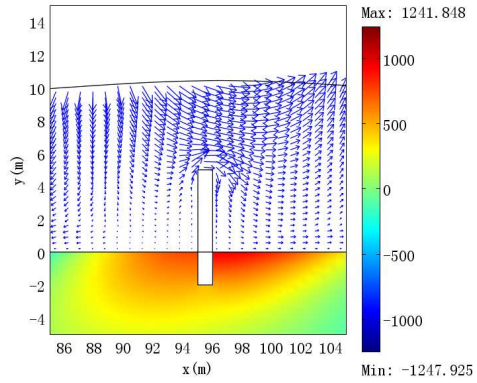

Figure 17. The sketch of velocity profile in the system of wave - vertical wall-soil interactions-Case 2(wave period=8s, wave height=0.5m).

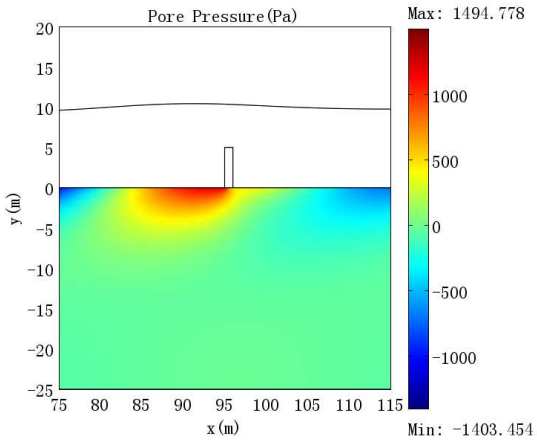

(a) Case 1

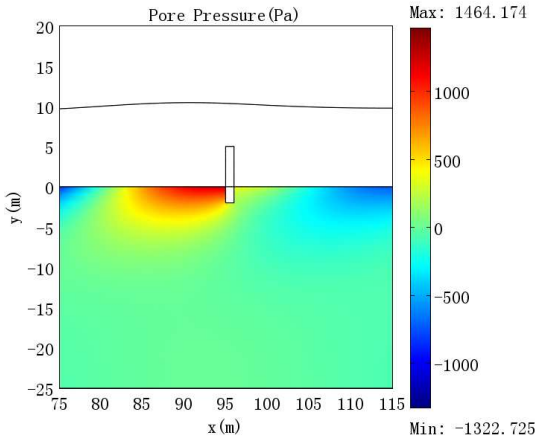

(b) Case 2

Figure 18. Effect of embedded depth of deformable structure on pore pressure.

In addition to the wave field and seabed, another new feature of this study is the structure components in the integrated model. Here, we consider the horizontal displacements at the top of the wall, which also indicate the oscillatory of the structure. It is noted the horizontal displacements presented here is generated by the wave loading, not artificial oscillating loading. As shown in Fig. 19, the patterns of the horizontal displacements at the top of the wall are similar for both cases. It is important to note that the horizontal displacement at the top of the wall in case 2 is two order higher than case 1. This implies that the design of case 2 can stand for two-order higher deformation of the pile than case 1.

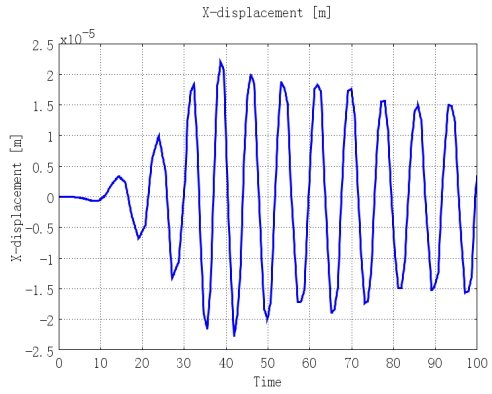

(a) Case 1

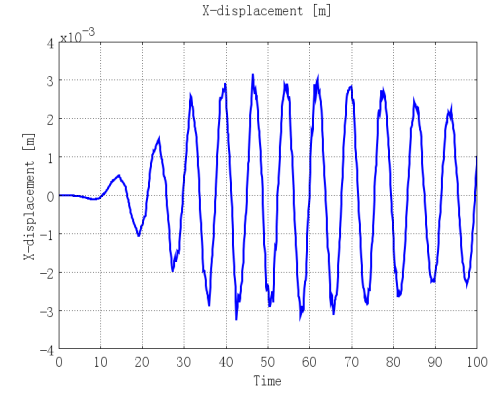

(b) Case 2

Figure 19. The horizontal displacements at the top of the wall (a) case 1 and (b) case 2

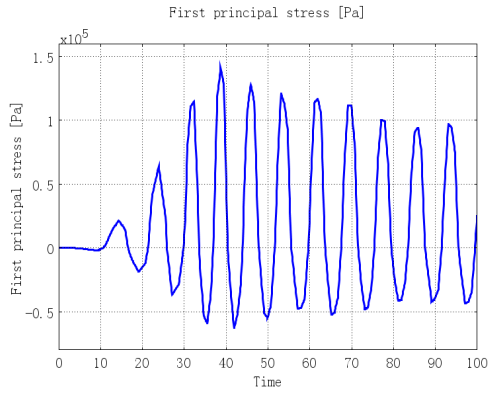

(a) Case 1

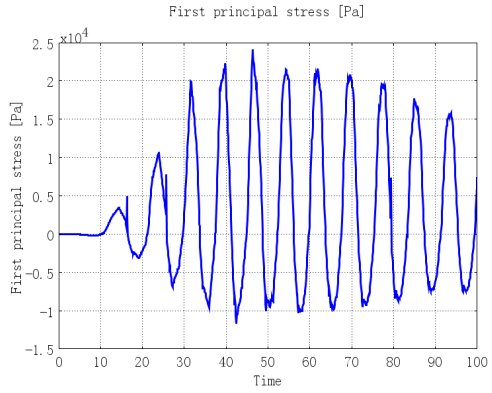

(b) Case 2

Figure 20. The first principal stress at point 1 (a) case 1 and (b) case 2

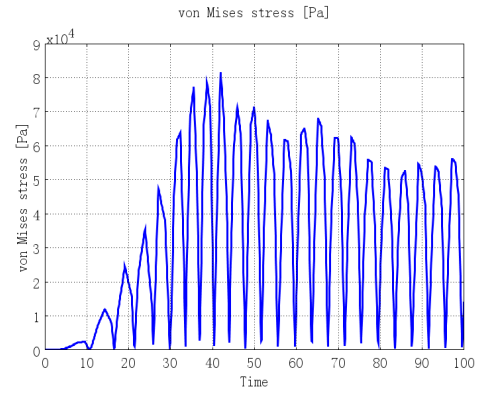

(a) Case 1

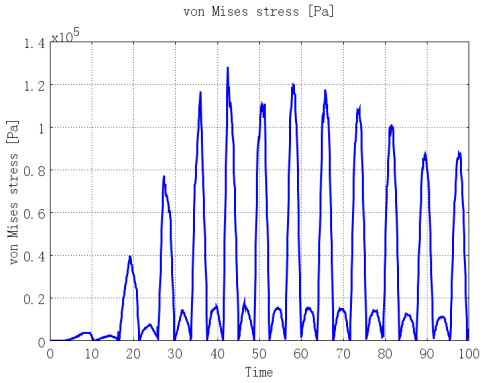

(b) Case 2

Figure 21. The von Mises stress at point 1(a) case 1 and (b) case 2

Figure 20 illustrates the first principal stress at point 1 (see Fig. 16) for both cases. As show in the figure, the first principal stresses at point 1 for case 1 is one-order higher than that in case 2. This implies that the bottom of the structure will received higher stresses in case 1, which required more intensive design for the structure. For von Mises stress at point 1 (Fig. 21), the highest vale is about 9×10^4 for case 1 and 1.2×10^5 for case 2. They can be considered as in the same order of magnitudes.

Based on results presented in Figs. 18 to 21, the design of case 2 provide a better design for the deformable pile in the wave-seabed-pile interaction system.

4. CONCLUSIONS

In this paper, we first present a new analytical solution for the wave/current-induced soil response in a porous seabed. Both oscillatory and residual mechanisms are considered in this study. Then, we present a numerical model for the simulations of wave propagating over a porous seabed around marine structures. Based on the numerical examples presented, the following conclusions can be drawn.

1. For the combined loading of waves and currents, the soil response increases as the current velocity increases.
2. A modified J-S Curve is established by including currents for the prediction of the liquefaction potential, which provides engineers a effective tool.
3. An integrated model, based on COMSOL Multiphysics, has been developed to study the WSSI phenomenon in this study. To validate this model, the simulated wave profile, pore fluid pressure and vertical effective normal stress in the case without any marine structure are compared with those from analytical theory. The comparison results show a good agreement between numerical simulation and analytical theory.
4. The numerical results show that the existence of a marine structure may significantly increase the wave crest height and its induced pore pressure within seabed.

5. The embedded depth of a deformable structure slightly affect the wave propagation but has a large impact on pore pressure around the structure foundation.

5. REFERENCES

Biot, M.A. 1941. General theory of three-dimensional consolidation. Journal of Applied Physics. 12(2):155–164.

Christian, J.T., Taylor, P.K., Yen, J.K.C. and Erali, D.R. 1974. Large diameter underwater pipeline for nuclear power plant designed against soil liquefaction. Proceeding of Offshore Technology Conference, Dallas. 597-606.

Dean, R. G. and Dalrymple, R. 1991. Water wave Mechanics for Engineers and Scientists, World Scientific.

Hsu, J.R.C., Jeng, D.S. and Tsai, C.P. 1993. Short-crested wave-induced soil response in a porous seabed of infinite thickness. International Journal for Numerical and Analytical Methods in Geomechanics. 17(8): 553–576.

Jeng, D.S. and Hsu, J. R. C. 1996. Wave-induced soil response in a nearly saturated seabed of finite thickness. Géotechnique. 46(3): 427–440.

Jeng, D. S. and Seymour, B.R. 2007. A simplified analytical approximation for pore-water pressure build-up in a porous seabed. Journal of Waterway, Port, Coastal and Ocean Engineering, ASCE. 133(4): 309–312.

Jeng, D. S. 1997. Wave-induced seabed response in front of a breakwater. PhD thesis, University of Western Australia.

Jeng, D. S. 2003. Wave-induced seafloor dynamics. Applied Mechanics Review. 56(4): 407–429.

Jeng, D. S., Cha, D.H., Lin, Y.S. and Hu, P.S. 2000. Analysis on pore pressure in a porous seabed in the vicinity of a caisson. Applied Ocean Research. 22: 317–329.

Lundgren, H., Lindhardt, J.H.C. and Romhild, C.J. 1989. Stability of breakwaters on porous foundation. Proceedings of 12th International Conference on Soil Mechanics and Foundation Engineering.1: 451-454.

Madga, W. 2000. Wave-induced cyclic pore-pressure perturbation effects in hydrodynamic uplift force acting on submarine pipeline buried in seabed sediments. Coastal Engineering. 39: 243–272.

Mase, H., Sakai, T., and Sakamoto, M. 1994. Wave-induced porewater pressure and effective stresses around breakwater. Ocean Engineering. 21: 361–379.

Mizutani, N., Mostafa, A.M. and Iwata, K. 1998. Nonlinear regular wave, submerged breakwater and seabed dynamic interaction. Coastal Engineering. 33: 177-202.

Nago, H., Maeno, S., Matsumoto, T. and Hachiman, Y. 1993. Liquefaction and densification of loosely deposited sand bed under water pressure variation. Proc of 3rd International Offshore and Polar Engineering Conf, Singapore. 578–584.

Sassa, S. and Sekiguchi, H. 1999. Wave-induced liquefaction of beds of sand in a centrifuge. Geotechnique. 49(5): 621–638.

Seed, H. B. and Rahman, M. S. 1978. Wave-induced pore pressure in relation to ocean floor stability of cohesionless soils. Marine Geotechnology. 3(2): 123–150.

Smith, A.W. and Gordon, A.D. 1983. Large breakwater toe failures, Journal of Waterway. Harbor and Coastal Engineering, ASCE. 109(2): 253-255.

Sumer, B. M. and Cheng, N. S. 1999. A random-walk model for pore pressure accumulation in marine soils. The 9th International Offshore and Polar Engineering Conf (ISOPE99), Brest France. 1: 521–528.

Sumer, B. M., Fredsoe, J. 2002. The Mechanics of Scour in the Marine Environment. World Scientific: Singapore. 536.

Yamamoto, T., Koning, H. L., Sellmejjer, H. and Hijum, E.V. 1978. On the response of a poro-elastic bed to water waves. Journal of Fluid Mechanics. 87: 193–206.

APPENDIX: WAVE AND CURRENT –INDUCED DYNAMIC PRESSURE

In this appendix, we provide detailed information of wave/current-induced dynamic pressure along the seabed surface. To satisfy the governing equation (1) and bottom boundary condition, we have velocity potential as:

$$\begin{aligned}\phi = &-U_0\left[(mm_1 - nn_1)x + (nm_1 + mn_1)y\right] \\ &+F\cosh kz\sin(mkx + nky - \omega t)\end{aligned} \tag{A1}$$

where A is an unknown coefficient and the water surface elevation as:

$$\eta = \frac{H}{2}\cos(mkx + nky - \omega t)\,, \tag{A2}$$

Substituting (A1) and (A2) into the dynamic free surface boundary (3), and take the linear terms, we have:

$$\begin{aligned}&F\omega\cosh kd\cos(mkx + nky - \omega t) \\ &\quad+\frac{1}{2}\left\{\left(mm_1 - nn_1\right)^2 U_0^2 - 2FU_0 mk(mm_1 - nn_1)\times\right. \\ &\qquad\left.\cosh kd\cos(mkx + nky - \omega t)\right\} \\ &\quad+\frac{1}{2}\left\{\left(nm_1 - mn_1\right)^2 U_0^2 - 2FU_0 nk(nm_1 + mn_1)\times\right. \\ &\qquad\left.\cosh kd\cos(mkx + nky - \omega t)\right\} \\ &\quad+\frac{gH}{2}\cos(mkx + nky - \omega t) = C\end{aligned} \tag{A3}$$

which leads to

$$F = \frac{-gH}{2\omega\left(1 - \dfrac{U_0 m_1 k}{\omega}\right)\cosh kd} \text{ and } C = \frac{U_0^2}{2} + gd \tag{A4}$$

Then, we have the velocity potential

$$\begin{aligned}\phi = &-U_0\left[(mm_1 - nn_1)x + (nm_1 + mn_1)y\right] \\ &-\frac{gH\cosh kz}{2\omega(1 - \dfrac{U_0 m_1 k}{\omega})\cosh kd}\sin(mkx + nky - \omega t)\end{aligned} \tag{A5}$$

Introducing (A3) and (A5) into kinematic boundary condition (4), we have the dispersion relation as:

$$\left(\omega - m_1 U_0 k\right)^2 = gk\tanh kd \tag{A6}$$

Which will be used to determine the wavelength $L = 2\pi/\lambda$.

$$\frac{P}{\rho} = g(d - z) + \frac{U_0^2}{2} + \frac{\partial\phi}{\partial t} - \frac{1}{2}\left[\left(\frac{\partial\phi}{\partial x}\right)^2 + \left(\frac{\partial\phi}{\partial y}\right)^2 + \left(\frac{\partial\phi}{\partial z}\right)^2\right] \tag{A7}$$

Again, taking the linear term, we have the dynamic wave pressure (P_d) as:

$$P_d = \frac{\gamma_w H}{2}\frac{\cosh kz}{\cosh kd}\cos(mkx + nky - \omega t)\,. \tag{A8}$$